Incorporation of *Mycobacterium tuberculosis* Lipoarabinomannan into Macrophage Membrane Rafts Is a Prerequisite for the Phagosomal Maturation Block[▽]

Amanda Welin, Martin E. Winberg, Hana Abdalla, Eva Särndahl,† Birgitta Rasmusson, Olle Stendahl, and Maria Lerm*

Medical Microbiology, Department of Clinical and Experimental Medicine, Faculty of Health Sciences, Linköping University, SE-58185 Linköping, Sweden

Lipoarabinomannan (LAM) is one of the key virulence factors for *Mycobacterium tuberculosis*, the etiological agent of tuberculosis. During uptake of mycobacteria, LAM interacts with the cell membrane of the host macrophage and can be detected throughout the cell upon infection. LAM can inhibit phagosomal maturation as well as induce a proinflammatory response in bystander cells. The aim of this study was to investigate how LAM exerts its action on human macrophages. We show that LAM is incorporated into membrane rafts of the macrophage cell membrane via its glycosylphosphatidylinositol anchor and that incorporation of mannose-capped LAM from *M. tuberculosis* results in reduced phagosomal maturation. This is dependent on successful insertion of the glycosylphosphatidylinositol anchor. LAM does not, however, induce the phagosomal maturation block through activation of p38 mitogen-activated protein kinase, contradicting some previous suggestions.

Mycobacterium tuberculosis, the etiological agent of tuberculosis, spreads by aerosol, mainly infecting alveolar macrophages, by which the bacterium is ingested (17). Through inhibition of macrophage functions, the bacterium modulates the host immune response (25). The best-characterized virulence factor of *M. tuberculosis*, lipoarabinomannan (LAM), is an abundant glycolipid, which is attached to the plasma membrane by a glycosylphosphatidylinositol (GPI) anchor and extends through the cell wall of the bacterium (5). During uptake of mycobacteria, LAM interacts with the cell membrane of the host macrophage via specific receptors, including the macrophage mannose receptor and complement receptor 3 (13, 14, 19), and can then be detected at multiple sites in the cell (27). The host cell exports LAM from the phagosome in an exocytosis-like manner, eliciting responses in bystander cells (1–3). The *M. tuberculosis* surface harbors mannose-capped LAM (ManLAM), whereas other, less pathogenic, mycobacteria contain LAM either with a phospho-*myo*-inositol cap (PILAM) or no cap (6). The type of capping and the presence of the GPI anchor is crucial for virulence (13, 14). The effects of ManLAM on the host cell are multiple, but the interference of ManLAM with phagosomal maturation is the best characterized (21) and has been demonstrated in murine and human macrophages (10, 12, 14).

Studies on human lymphocytes showed that LAM localizes to membrane rafts of the lymphocyte membrane, thereby interfering with signaling affecting cytokine production (20).

Membrane rafts are cholesterol- and glycosphingolipid-rich domains that act as platforms for cell signaling processes (16). The aim of this study was to investigate whether the effects of LAM are due to incorporation of LAM into membrane rafts of human macrophages. We establish that LAM is incorporated into membrane rafts of the macrophage cell membrane via its GPI anchor, resulting in reduced phagosomal maturation.

MATERIALS AND METHODS

Antigens and antibodies. ManLAM, cell wall fractions (CWF), and phosphatidylinositol mannosides (PIM) from the virulent *M. tuberculosis* strain H37Rv; PILAM from an avirulent strain; and monoclonal anti-LAM antibodies were kindly provided by Colorado State University, Fort Collins, CO. Mouse monoclonal CD63 antibody was from Sanquin, rabbit monoclonal phospho-p38 mitogen-activated protein kinase (MAPK) antibody (Thr180/Tyr182) was from Cell Signaling Technology, and the mouse monoclonal p65 antibody was from Santa Cruz. Alexa 594- and Alexa 488-conjugated goat anti-mouse immunoglobulin G (IgG) and Alexa 594-conjugated goat anti-rabbit IgG were from Molecular Probes, and horseradish peroxidase (HRP)-conjugated goat anti-rabbit and goat anti-mouse antibodies were from Dako.

Cell culture. Human monocytes were isolated from heparinized peripheral human blood by routine methods. Briefly, whole blood was layered onto Lymphoprep (Axis-Shield) and centrifuged at $480 \times g$ at room temperature (RT) for 40 min. The mononuclear cell layer was collected and washed several times. Cells were seeded on glass coverslips or plastic and diluted in cold Dulbecco's modified Eagle's medium with glucose (Gibco) (supplemented with 20 mM HEPES, 1 U/ml penicillin, 10 μg/ml streptomycin); lymphocytes were washed away after 1 to 2 h, and cells were allowed to differentiate into human monocyte-derived macrophages (hMDMs) for 8 to 11 days in the same medium containing 10% normal human serum pooled from five donors (Linköping University Hospital) and 80 μM L-glutamine. The day before experiment, the medium was replaced with serum-free medium.

LAM and PIM loading. Macrophages were loaded (at 37°C for 30 min on a rocking table) with ManLAM (5 μg/ml or 20 μg/ml), PILAM (5 μg/ml or 20 μg/ml), CWF (20 μg/ml or 80 μg/ml), PIM (20 μg/ml or 40 μg/ml), or control (buffer only) diluted in Krebs-Ringer glucose medium (120 mM NaCl, 4.9 mM KCl, 1.2 mM $MgSO_4$, 8.3 mM KH_2PO_4, 10 mM glucose, 1 mM $CaCl_2$). After incubation, the cells were washed three times to remove unbound LAM. In order

* Corresponding author. Mailing address: Medical Microbiology, Linköping University, SE-58185 Linköping, Sweden. Phone: 4613224779. Fax: 4613224789. E-mail: marle@imk.liu.se.

† Present address: Department of Biomedicine, School of Health and Medical Sciences, Örebro University, SE-701 82 Örebro, Sweden.

to competitively inhibit LAM insertion (13), macrophages were incubated with PIM for 15 min before, as well as during, LAM incubation.

LAM staining. After LAM loading (20 μg/ml), hMDMs were fixed in 4% paraformaldehyde (PFA) for 30 min and washed three times. Cells were blocked (at RT for 1 h) with phosphate-buffered saline (PBS) with 5% human serum albumin and then incubated (at RT for 1 h) with monoclonal anti-LAM (cs-35) antibody (1:50) in blocking buffer containing 0.5% human serum albumin supplemented with 10% normal goat serum (Dako). After three 5-min washes, cells were incubated (at RT for 1 h) with Alexa 594-conjugated anti-mouse IgG (5 μg/ml) diluted in blocking solution. After three additional washes, the coverslips were mounted (Dako mounting medium), and preparations were analyzed by confocal microscopy. The confocal microscope was a Bio-Rad Radiance 2000 MP with LaserSharp 2000 software with an argon laser emitting dually at 488 nm for excitation of green fluorescence and at 514 nm for red fluorescence. For double immunofluorescent labeling of LAM and ganglioside M-1 (GM-1), a molecule remaining in the detergent-resistant membrane raft fraction of membranes, the preparations were incubated with the Alexa-conjugated B subunit of cholera toxin (1 μg/ml; at 4°C for 15 min) (Molecular Probes) before fixation and LAM staining.

Membrane raft isolation. After LAM loading, macrophages were incubated (at 4°C for 30 min) in cold lysis buffer (1 mM EDTA; 1% Triton X-100; 2 μg/ml each of aprotinin, pepstatin, and leupeptin; 1 mM Pefabloc [Roche]). Lysates were centrifuged (at $500 \times g$ at RT for 10 min) to remove nuclei and whole cells, and supernatants were mixed 1:1 with 85% sucrose (wt/vol) diluted in lysis buffer. A step gradient of 30% sucrose and 5% sucrose was constructed on top of the mixture and ultracentrifuged ($200,000 \times g$ at 4°C for 18 h). Ten fractions (1 ml each) were collected from the top to the bottom of the tube, transferred to a nitrocellulose membrane by dot blot, and blocked for 1 h at RT with 5% (wt/vol) fat-free milk. GM-1 was detected using the HRP-conjugated B subunit of cholera toxin (1 μg/ml; at RT for 1 h) (Sigma-Aldrich), and LAM was detected using mouse monoclonal anti-LAM antibody (1:200; at RT for 2 h) followed by HRP-conjugated goat anti-mouse antibody (1:5,000; at RT for 1 h). Dots were detected using a commercial kit (Amersham Bioscience).

CD63 translocation assay. LAM-loaded or control hMDMs were allowed to phagocytose (15 min) fluorescein isothiocyanate-labeled serum-opsonized zymosan particles (10:1) (Sigma-Aldrich). After a washing step, phagosomal maturation was allowed to proceed (at 37°C for 2 h). hMDMs were fixed in PFA and washed three times. Staining of the lysosomal marker CD63, which is found on mature phagosomes (9), was performed in a humid chamber. Briefly, cells were blocked in blocking solution containing PBS with 2% bovine serum albumin and 10% normal goat serum and permeabilized (at RT for 30 min) in blocking solution supplemented with 0.1% (wt/vol) saponin. After three washes in PBS, cells were incubated (at RT for 1 h) with mouse monoclonal anti-CD63 antibody (4 μg/ml) diluted in blocking solution. After three 5-min washes, cells were incubated (at 37°C for 30 min) with Alexa 594-conjugated goat anti-mouse IgG (5 μg/ml), also diluted in blocking solution. Coverslips were washed three times and mounted, and preparations were coded to achieve unbiased analysis, upon which they were analyzed with respect to CD63 staining.

LysoTracker assay. LAM-loaded and control macrophages in Delta-T dishes (Bioptechs) were allowed to phagocytose (15 min) fluorescent latex beads (Fluoresbrite plain YG 2.0 micron microspheres; Polysciences) at a multiplicity of infection of 10:1. After a washing step, phagosomal maturation was allowed to proceed for 2 h. When 15 min of incubation remained, 75 nM LysoTracker Red DND-99 (Molecular Probes) was added. Cells were washed and mounted in a confocal microscope equipped with a temperature control unit set to 37°C. At least 30 images were taken of each of the coded samples during the following 45-min period, and the images were analyzed with respect to LysoTracker localization to the phagosome. Each treatment was started separately so that the incubation time was equal for all samples.

Phosphorylation of p38 MAPK. After ManLAM loading (20 μg/ml), hMDMs were either stimulated with serum-opsonized zymosan (5:1) at 37°C for 20 min or left untreated and washed three times. Cold radioimmunoprecipitation assay buffer (1% Triton X-100, 0.1% sodium dodecyl sulfate [SDS], 0.5% sodium deoxycholate, 9.1 mM dibasic sodium phosphate, 1.7 mM monobasic sodium phosphate, 150 mM NaCl), supplemented with Complete mini protease inhibitor cocktail (Roche), 1 mM Na-ortovanadate, and 5 μM dithiothreitol, was added at 4°C for 10 min; samples were centrifuged ($10,000 \times g$ at 4°C for 10 min), and the supernatant was diluted with sample buffer. Samples of equal protein content were subjected to SDS-polyacrylamide gel electrophoresis and transferred to a polyvinylidene difluoride membrane, which was blocked with 5% bovine serum albumin (at RT for 1 h). Phosphorylation of p38 MAPK was detected by means of enhanced chemiluminescence using an anti-phospho-p38 antibody (1:1,000; at 4°C overnight) and a secondary HRP-conjugated anti-rabbit antibody (1:2,000; at

RT for 2 h). The blots were scanned, and the relative intensities of the bands were quantified using ImageJ, version 1.37, software.

NF-κB assay. hMDMs were exposed to 20 μg/ml LAM as described above or left untreated prior to the addition of Toll-like receptor 2 (TLR2) ligand (Pam$_3$Cys) or TLR4 ligand (lipopolysaccharide [LPS]) (Alexis), 50 ng/ml or 10 ng/ml, respectively, in Krebs-Ringer glucose medium with 1% normal human serum. After incubation at 37°C for 15 min, the cells were fixed with PFA, and NF-κB activation was assessed by immunofluorescence staining. In brief, the cells were stained with a monoclonal antibody directed toward the p65-subunit of NF-κB, which translocates into the nucleus upon activation, and an Alexa 594-conjugated anti-mouse antibody. The preparations were mounted in mounting medium and analyzed with a Zeiss Axiovert 200 microscope equipped with an AxioCamMRm camera. The staining intensity of the nucleus versus the cytoplasm was measured in at least 50 cells using Scion Image, version 4.0.2, software, and NF-κB activation was expressed as the ratio of nuclear to cytoplasmic staining.

Analysis. A Student's t test was used for statistical analysis, and P values of ≤0.05 were considered significant. A Kolmogorov-Smirnov test was used to ensure that data were normally distributed.

RESULTS

LAM is incorporated into the cell membrane of hMDMs and localizes to membrane rafts. In order to investigate whether LAM is incorporated into the cell membrane of primary human macrophages, the cells were incubated with LAM. LAM-specific staining of hMDMs was elevated in the Man-LAM-containing samples, compared to PILAM, PIM, PIM/ManLAM, and controls (Fig. 1A). To elucidate whether LAM localizes to membrane rafts in hMDMs, dot blot analysis of cell fractions of LAM-treated and control cells was performed. As depicted in Fig. 1B, the raft marker GM-1 is present in fractions 7 and 8 from control cells. The localization of GM-1 is not altered in LAM-treated cells, showing that rafts are not disrupted by LAM. Immunodetection of LAM in LAM-treated cells showed that LAM localizes to the same fractions as GM-1 (Fig. 1B, fractions 7 and 8), indicating that LAM is incorporated into the cell membrane and localizes to membrane rafts upon interaction with hMDMs. PILAM, from an avirulent mycobacterial strain, is also incorporated into membrane rafts but to a lesser extent. One previous study established that incubation of PIM simultaneously with LAM competitively inhibits LAM insertion, as PIM is structurally identical to the GPI anchor of LAM (13). LAM staining is notably reduced in PIM/LAM-treated cells, showing that LAM insertion is competitively inhibited by simultaneous PIM treatment. Quantification of staining intensity showed that PIM blocks LAM insertion by about 50%. Double fluorescent labeling of LAM and GM-1 confirmed colocalization (Fig. 1C).

ManLAM reduces phagosomal maturation. The best-characterized function of LAM is its ability to inhibit phagosomal maturation although no study has investigated whether this effect is due to incorporation of LAM into the host cell membrane. Since the phagosomal membrane originates from the plasma membrane and since membrane rafts are present on the phagosome, we concluded that LAM is present in the phagosomal membrane of LAM-loaded hMDMs (8). LAM-treated or control hMDMs were allowed to ingest fluorescein isothiocyanate-labeled, serum-opsonized zymosan particles. To assess the process of phagosomal maturation, the translocation of the lysosomal marker CD63 to the phagosomes of the fixed hMDMs was examined in an unbiased manner. Analysis of confocal images was performed by scoring phagosomes as
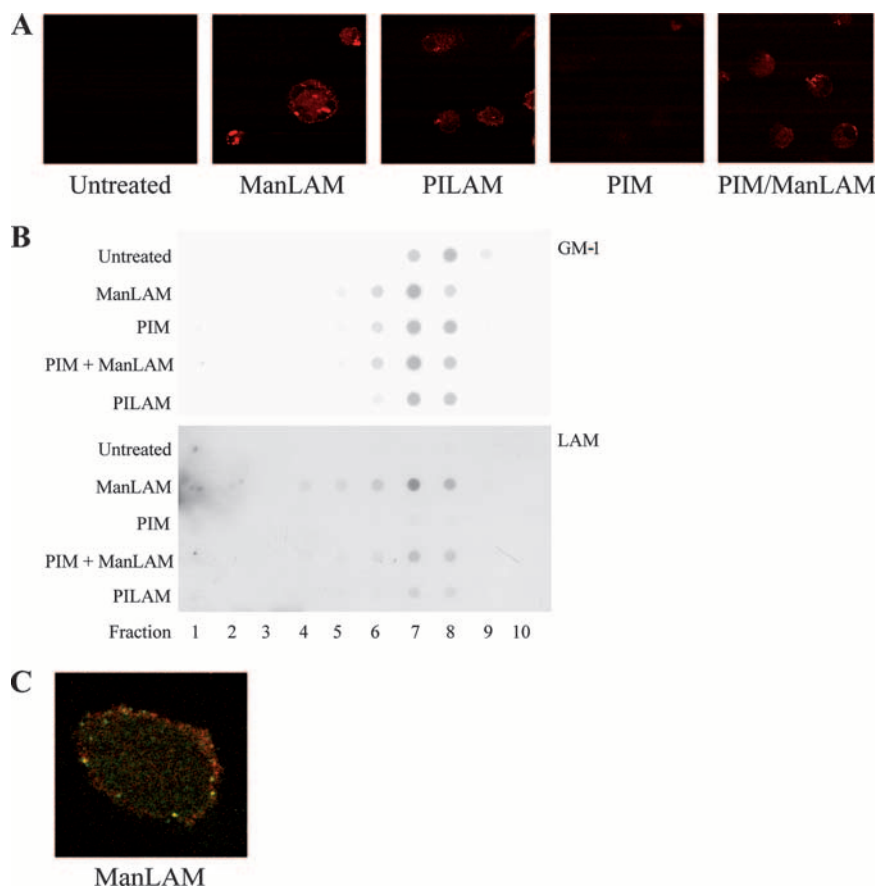
FIG. 1. Distribution of LAM in hMDMs. (A) Macrophages were incubated with the glycolipids (20 μg/ml), immunostained for LAM, and analyzed by confocal microscopy. The confocal images show representative examples of control cells and cells treated with ManLAM, PILAM, PIM, and PIM/ManLAM. Red staining in the cell periphery denotes the presence of LAM. (B) The cell membranes of untreated hMDMS and of hMDMs treated with ManLAM (20 μg/ml), PIM (20 μg/ml), PIM+ManLAM (20 μg/ml of each) and PILAM (20 μg/ml) were separated by sucrose gradient fractionation; the fractions were transferred to nitrocellulose and stained with the HRP-conjugated B subunit of cholera toxin for GM-1, which is a marker of detergent-resistant membranes (upper panel), or a monoclonal anti-LAM antibody followed by an HRP-conjugated secondary antibody (lower panel). The dot blots show fractions 1 to 10 (bottom to top) of the macrophage cell membrane. For the top panel, the intensity has been decreased by 5 units in Adobe Photoshop. (C) hMDMs were subjected to double labeling of LAM (green) and GM-1 (red). The confocal image shows a representative ManLAM-treated cell.

positive or negative for CD63 translocation. Figure 2A depicts representative images of phagosomes positive and negative for CD63 translocation. Quantification of the translocation of CD63 to the phagosome showed that incorporation of ManLAM and CWF (of which LAM is an abundant component), but not PILAM, inhibits the translocation of CD63 to phagosomes after 2 h of phagosomal maturation (Fig. 2B). The inhibition is significant for both the lower and higher concentrations of ManLAM ($P = 0.012$ and $P < 0.0001$, respectively) and for both the higher and lower concentrations of CWF ($P = 0.05$ and $P = 0.021$, respectively). PILAM, however, did not alter phagosomal maturation significantly. The results for ManLAM were confirmed using a LysoTracker-based method, where ManLAM-loaded hMDMs were allowed to phagocytose fluorescent latex beads. Figure 3A depicts representative images of phagosomes positive and negative for LysoTracker, which localizes to acidic granules. Quantification of LysoTracker presence around the phagosome showed that ManLAM inhibits phagosomal acidification (Fig. 3B).

PIM treatment reverses the effect of LAM. In order to see if insertion of the GPI anchor of LAM is a prerequisite for phagosomal maturation inhibition, PIM was added during LAM treatment, and the CD63 translocation assay was performed. PIM on its own had a slight but nonsignificant inhibitory effect on phagosomal maturation ($P = 0.093$) although this effect was not as pronounced as with ManLAM ($P < 0.0001$) (Fig. 2C). When added during LAM treatment, PIM ($P = 0.041$) reversed the inhibitory effect of LAM, which was reduced to the level of PIM alone (Fig. 2C).

LAM does not activate p38 MAPK in hMDMs. Studies on mouse macrophage cell lines have suggested that the effect of *M. tuberculosis* on phagosomal maturation is partly due to activation of p38 MAPK (9, 23, 25), and it is known that the attenuated *M. tuberculosis* strain H37Ra activates p38 MAPK in human neutrophils (15). To investigate the effects of LAM on p38 MAPK, cells were pretreated with ManLAM and/or opsonized zymosan, which is known to activate p38. LAM did not induce p38 MAPK activation, nor did
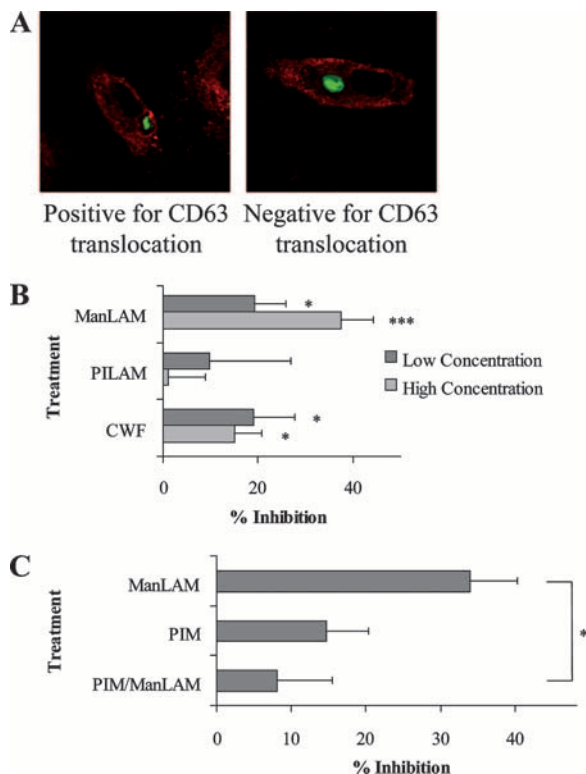
FIG. 2. Effect of LAM on CD63 translocation to phagosomes. Control hMDMs and hMDMs preincubated with ManLAM, PILAM, or CWF were allowed to phagocytose zymosan particles. After 2 h of incubation, CD63 was immunostained. Phagosomes in recoded samples were classified as positive or negative for CD63 translocation. (A) Confocal images showing representative phagosomes classified as positive or negative for CD63 translocation. Red staining around the green zymosan particle indicates CD63 translocation. (B) Histogram showing the percent inhibition of CD63 translocation to the phagosome, compared to control, in the differently treated hMDMs. Dark bars represent the lower loading concentrations (5 μg/ml for ManLAM and PILAM and 20 μg/ml for CWF), and light bars represent the higher loading concentrations (20 μg/ml for ManLAM and PILAM and 80 μg/ml for CWF). The graph represents the average of 10 (ManLAM), 4 (PILAM), or 7 (CWF) independent experiments in which at least 40 phagosomes were classified per sample. A statistically significant difference from the control is denoted as follows: *, $P \leq 0.05$; ***, $P < 0.0001$. (C) Histogram showing the effect of PIM on LAM insertion. hMDMs preincubated with PIM (40 μg/ml) or ManLAM (20 μg/ml) alone or with PIM together with ManLAM were allowed to phagocytose zymosan particles. After 2 h of incubation, CD63 was immunostained. Phagosomes were classified as positive or negative for CD63 translocation in an unbiased manner. The histogram shows the percent inhibition of CD63 translocation to the phagosome, compared to control, in the differently treated hMDMs. The graph represents the average of 10 (ManLAM) or 3 (PIM) independent experiments in which at least 40 phagosomes were classified per sample. A significant difference from ManLAM is denoted by an asterisk ($P \leq 0.05$). Error bars show the standard errors of the means.

LAM interfere with the p38 activation achieved through phagocytosis of opsonized particles, as shown in Fig. 4A and B.

LAM incorporation into membrane rafts does not interfere with TLR2 or TLR4 signaling. Knowing that LAM localizes to membrane rafts and inhibits phagosomal maturation, we aimed at investigating whether the function of TLR2 and TLR4, which have been linked to phagosomal maturation (4),
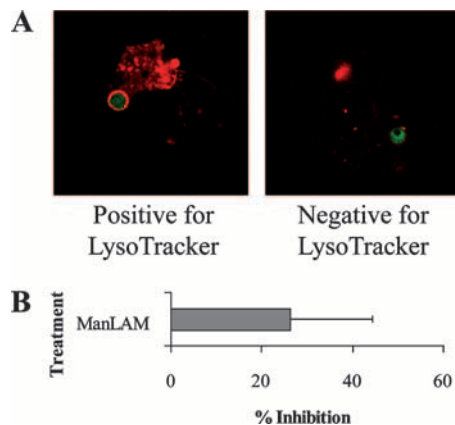
FIG. 3. Effect of ManLAM on phagosomal acidification. Control hMDMs and hMDMs preincubated with ManLAM (20 μg/ml) were allowed to phagocytose fluorescent beads and were incubated for 2 h. When 15 min remained, LysoTracker Red DND-99 was added, and preparations were analyzed using a confocal microscope. Phagosomes in recoded samples were classified as positive or negative for Lyso-Tracker presence around the phagosome. (A) Confocal images showing representative phagosomes classified as positive or negative for LysoTracker presence, as indicated by red staining around the green bead. (B) Histogram showing the percent inhibition of phagosomal acidification, compared to control, in ManLAM-treated hMDMs. At least 40 phagosomes were classified per sample in two independent experiments. The error bar shows standard error of the mean.

is disturbed by the incorporation of mycobacterial lipids into membrane rafts. hMDMs were exposed to ManLAM prior to the addition of TLR2 and TLR4 ligands (Pam_3Cys and LPS, respectively). After incubation, the cells were fixed, and NF-κB translocation was analyzed as a measure of TLR function. The ratio of nuclear versus cytoplasmic staining intensity of NF-κB
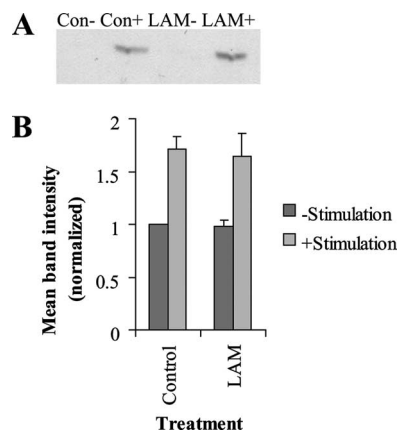
FIG. 4. Phosphorylation of p38 MAPK in LAM-treated hMDMs. Cells were incubated with 20 μg/ml LAM and stimulated with opsonized zymosan or left untreated, as indicated. Cell lysates were subjected to SDS-polyacrylamide gel electrophoresis, processed for Western blotting, and stained for phosphorylated p38 MAPK. (A) A representative blot showing the p38 MAPK bands. The contrast has been increased by 40 units in Adobe Photoshop. (B) Blots were scanned, and the relative intensities of the bands were quantified and normalized against the control. The histogram shows the mean relative intensities of the bands. Error bars show the standard errors of the means. The histogram is the result of three independent experiments. Con, control.
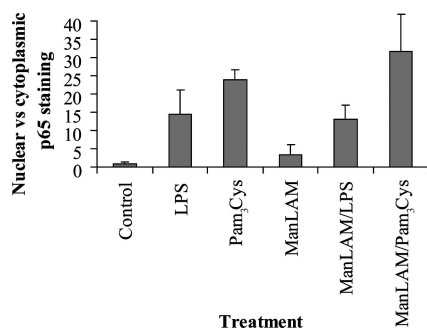
FIG. 5. Effect of LAM on NF-κB activity in hMDMs. Macrophages were pretreated with ManLAM and stimulated with LPS or Pam₃Cys. Fixed cells were stained with an antibody directed toward the p65 subunit of NF-κB and a fluorescent secondary antibody. Images were obtained by fluorescence microscopy of the cells, and activity of NF-κB was assessed as the ratio of nuclear versus cytoplasmic p65 staining. A total of 30 to 43 cells per preparation were analyzed, and the error bars show standard errors of the means. The presented data are from one measurement that is representative of three independent experiments.

was slightly enhanced by LAM-treatment (Fig. 5). However, pretreatment with LAM did not prevent the strong activation of NF-κB induced by Pam₃Cys or LPS, indicating that signaling from TLR2 and TLR4 is intact in LAM-treated cells. Instead, some additive effect of LAM and Pam₃Cys was observed (Fig. 5).

DISCUSSION

In recent years, LAM has been repeatedly highlighted as a major contributor to *M. tuberculosis* virulence. Using confocal microscopy and dot blot analysis, we now show that LAM is incorporated into the cell membrane of macrophages upon incubation. Our model mimics the shedding of LAM from mycobacteria (27). Spontaneous incorporation of LAM has been observed by others (13, 20). Several studies on the effects of LAM on phagosomal maturation are based on the use of latex beads coated with LAM (10, 14). However, none of these dealt with whether the action of LAM is linked to its insertion since precoating of the latex beads with LAM does not allow examination of the site of LAM action. The present study shows that the effect of LAM on phagosomal maturation is preceded by the insertion of the glycolipid into rafts of the host cell membrane. Whether this occurs at the cell membrane level or in the phagosome during phagocytosis of mycobacteria is not clear.

The affinity of LAM for membrane rafts has previously been shown in human T helper cells (20) and in P1798 lymphoma cells (13), where the affinity of mycobacterial LAM for membrane rafts leads to modulation of signal transduction pathways. Shabaana et al. (20) find that LAM, when successfully inserted into rafts through the GPI anchor, has a transbilayer effect on the raft signaling platform, leading to functional alterations on raft protein kinases and ultimately modification of cytokine production. We find that PIM blocks LAM incorporation into hMDM membrane rafts, which is consistent with a previous study (13), and this is likely due to the structural similarity between the GPI anchor of LAM and PIM.

The present study shows that maturation of phagosomes in hMDMs carrying ManLAM in their membranes is significantly

reduced. This finding is supported by other studies using latex beads, as reviewed by Deretic et al. (7). CWF, which contains large amounts of ManLAM but also other components, had an effect similar to that of ManLAM. Additionally, our results show that PILAM from avirulent mycobacteria does not affect phagolysosomal fusion, which is also consistent with previous studies using the latex bead model (14). Kang et al. (14) suggest that interactions between ManLAM and the mannose receptor direct the phagocytic particles to a compartment that is less likely to mature. PILAM does not contain the mannose cap and thus cannot interact with the mannose receptor. In fact, PILAM binding via TLR2 induces a proinflammatory response, while ManLAM binding via mannose receptors elicits an anti-inflammatory response (14). We also observed that ManLAM does not block phagosomal maturation completely. A possible explanation for this is that not all bacteria manage to escape phagosomal maturation or that other mycobacterial components are necessary for an efficient block (18). Alternatively, escape from phagosomal maturation is only part of the *M. tuberculosis* strategy of survival in the macrophage.

Inhibition of LAM incorporation through PIM abrogates the effect of ManLAM on phagosomal maturation, indicating that the insertion of the glycolipid into the cell membrane is essential for the effect of LAM. PIM on its own has a tendency to inhibit phagosomal maturation yet to a lower extent than LAM. Since PIM and LAM have a structurally identical GPI anchor and since we show that it is insertion of the GPI anchor that mediates the phagosomal maturation block, this result could be expected. The inhibitory effect of PIM on phagosomal maturation was actually previously reported by Vergne and colleagues (26) although that study did not compare the effects of PIM and LAM. We find that PILAM is inserted less efficiently into the cell membrane of hMDMs than ManLAM, and this is probably the reason why PILAM does not block phagosomal maturation.

Inhibition of phagosomal maturation by *M. tuberculosis* has previously been explained in part by the inhibition of a rise in cytosolic Ca^{2+} and subsequent p38 MAPK activation, resulting in the failure to recruit early endosomal antigen 1, which is necessary for delivery of lysosomal components to the maturing phagosome (25). *Mycobacterium bovis* bacille Calmette-Guérin or *M. tuberculosis* infection activates p38 MAPK in mouse macrophages and human neutrophils, respectively (9, 15). However, the effect of isolated LAM on p38 has not been investigated previously, and our data show that LAM does not trigger the p38 pathway. The data suggest that other mycobacterial components act via this pathway.

The role of p38 in phagosomal maturation is unclear. Some studies indicate that p38 activation enhances phagosomal maturation (4), whereas others show that activation of p38 blocks this process (9). Vergne et al. suggested that activation of p38 is one mechanism by which *M. tuberculosis* blocks phagosomal maturation (25). Our results do not allow conclusions on the role of p38 in phagosomal maturation but clearly show that LAM neither activates nor blocks activation of p38. The activation of p38 observed with *M. tuberculosis* may be triggered by other components of the bacterium (9, 15, 23). In a recent study, Hayakawa et al. (11) observed that LAM modulates lipid membrane domain morphology and that membrane reorganization leads to inhibition of vesicle fusion as the reor-

ganized phagosomal membrane no longer has access to molecules essential for phagosomal maturation, for example, early endosomal antigen 1. This model offers an alternative explanation for the incorporation-dependent effect of LAM on phagosomal maturation we observed here.

TLRs are activated by a number of bacterial and viral products, which trigger the homo- or heterodimerization of the receptors in membrane rafts (22). The rafts then act as the signaling platform for the TLRs to induce an inflammatory response by activating NF-κB. Blander and Medzhitov (4) showed that TLR activation enhances phagosomal maturation although this finding has been questioned by other studies (28). In our model system, we used zymosan particles that by activating TLR2 (24) would secure efficient phagosomal maturation in the control experiment. To elucidate whether LAM treatment would alter TLR signaling, we investigated whether TLR2- and TLR4-mediated NF-κB activation was functional in LAM-treated cells. Our data show that ManLAM alone causes a slight activation of NF-κB. However, pretreatment of cells with LAM did not reduce the NF-κB response induced by TLR2 or TLR4 ligands, indicating that incorporation of LAM into the plasma membrane of hMDMs does not affect TLR function.

We found that *M. tuberculosis* LAM is incorporated into the cell membrane of human hMDMs and that LAM localizes to membrane rafts. Here, ManLAM interferes with phagosomal maturation in a manner dependent on insertion of its GPI anchor. Our unpublished data suggest a similar mechanism for the *Leishmania donovani* glycolipid lipophosphoglycan. However, LAM does not disrupt membrane rafts, activate p38 MAPK, or interfere with TLR signaling.

ACKNOWLEDGMENTS

REFERENCES

1. Beatty, W. L., E. R. Rhoades, H. J. Ullrich, D. Chatterjee, J. E. Heuser, and D. G. Russell. 2000. Trafficking and release of mycobacterial lipids from infected macrophages. Traffic 1:235–247.
2. Beatty, W. L., and D. G. Russell. 2000. Identification of mycobacterial surface proteins released into subcellular compartments of infected macrophages. Infect. Immun. 68:6997–7002.
3. Bhatnagar, S., K. Shinagawa, F. J. Castellino, and J. S. Schorey. 2007. Exosomes released from macrophages infected with intracellular pathogens stimulate a proinflammatory response in vitro and in vivo. Blood 110:3234–3244.
4. Blander, J. M., and R. Medzhitov. 2004. Regulation of phagosome maturation by signals from Toll-like receptors. Science 304:1014–1018.
5. Briken, V., S. A. Porcelli, G. S. Besra, and L. Kremer. 2004. Mycobacterial lipoarabinomannan and related lipoglycans: from biogenesis to modulation of the immune response. Mol. Microbiol. 53:391–403.
6. Dao, D. N., L. Kremer, Y. Guerardel, A. Molano, W. R. Jacobs, Jr., S. A. Porcelli, and V. Briken. 2004. *Mycobacterium tuberculosis* lipomannan induces apoptosis and interleukin-12 production in macrophages. Infect. Immun. 72:2067–2074.
7. Deretic, V., S. Singh, S. Master, J. Harris, E. Roberts, G. Kyei, A. Davis, S. de Haro, J. Naylor, H. H. Lee, and I. Vergne. 2006. *Mycobacterium tuberculosis* inhibition of phagolysosome biogenesis and autophagy as a host defence mechanism. Cell Microbiol. 8:719–727.
8. Dermine, J. F., S. Duclos, J. Garin, F. St-Louis, S. Rea, R. G. Parton, and M. Desjardins. 2001. Flotillin-1-enriched lipid raft domains accumulate on maturing phagosomes. J. Biol. Chem. 276:18507–18512.
9. Fratti, R. A., J. Chua, and V. Deretic. 2003. Induction of p38 mitogen-activated protein kinase reduces early endosome autoantigen 1 (EEA1) recruitment to phagosomal membranes. J. Biol. Chem. 278:46961–46967.
10. Fratti, R. A., J. Chua, I. Vergne, and V. Deretic. 2003. *Mycobacterium tuberculosis* glycosylated phosphatidylinositol causes phagosome maturation arrest. Proc. Natl. Acad. Sci. USA 100:5437–5442.
11. Hayakawa, E., F. Tokumasu, G. A. Nardone, A. J. Jin, V. A. Hackley, and J. A. Dvorak. 2007. A *Mycobacterium tuberculosis*-derived lipid inhibits membrane fusion by modulating lipid membrane domains. Biophys. J. 93:4018–4030.
12. Hmama, Z., K. Sendide, A. Talal, R. Garcia, K. Dobos, and N. E. Reiner. 2004. Quantitative analysis of phagolysosome fusion in intact cells: inhibition by mycobacterial lipoarabinomannan and rescue by an 1α,25-dihydroxyvitamin D3-phosphoinositide 3-kinase pathway. J. Cell Sci. 117:2131–2140.
13. Ilangumaran, S., S. Arni, M. Poincelet, J. M. Theler, P. J. Brennan, Nasir-ud-Din, and D. C. Hoessli. 1995. Integration of mycobacterial lipoarabinomannans into glycosylphosphatidylinositol-rich domains of lymphomonocytic cell plasma membranes. J. Immunol. 155:1334–1342.
14. Kang, P. B., A. K. Azad, J. B. Torrelles, T. M. Kaufman, A. Beharka, E. Tibesar, L. E. DesJardin, and L. S. Schlesinger. 2005. The human macrophage mannose receptor directs *Mycobacterium tuberculosis* lipoarabinomannan-mediated phagosome biogenesis. J. Exp. Med. 202:987–999.
15. Perskvist, N., L. Zheng, and O. Stendahl. 2000. Activation of human neutrophils by *Mycobacterium tuberculosis* H37Ra involves phospholipase Cγ2, Shc adapter protein, and p38 mitogen-activated protein kinase. J. Immunol. 164:959–965.
16. Pike, L. J. 2006. Rafts defined: a report on the Keystone Symposium on Lipid Rafts and Cell Function. J. Lipid Res. 47:1597–1598.
17. Russell, D. G. 2001. *Mycobacterium tuberculosis*: here today, and here tomorrow. Nat. Rev. Mol. Cell Biol. 2:569–577.
18. Russell, D. G., G. E. Purdy, R. M. Owens, K. H. Rohde, and R. M. Yates. 2005. *Mycobacterium tuberculosis* and the four-minute phagosome. ASM News 71:459–463.
19. Schlesinger, L. S. 1993. Macrophage phagocytosis of virulent but not attenuated strains of *Mycobacterium tuberculosis* is mediated by mannose receptors in addition to complement receptors. J. Immunol. 150:2920–2930.
20. Shabaana, A. K., K. Kulangara, I. Semac, Y. Parel, S. Ilangumaran, K. Dharmalingam, C. Chizzolini, and D. C. Hoessli. 2005. Mycobacterial lipoarabinomannans modulate cytokine production in human T helper cells by interfering with raft/microdomain signalling. Cell Mol. Life Sci. 62:179–187.
21. Strohmeier, G. R., and M. J. Fenton. 1999. Roles of lipoarabinomannan in the pathogenesis of tuberculosis. Microbes Infect. 1:709–717.
22. Triantafilou, M., F. G. Gamper, R. M. Haston, M. A. Mouratis, S. Morath, T. Hartung, and K. Triantafilou. 2006. Membrane sorting of Toll-like receptor (TLR)-2/6 and TLR2/1 heterodimers at the cell surface determines heterotypic associations with CD36 and intracellular targeting. J. Biol. Chem. 281:31002–31011.
23. Tse, H. M., S. I. Josephy, E. D. Chan, D. Fouts, and A. M. Cooper. 2002. Activation of the mitogen-activated protein kinase signaling pathway is instrumental in determining the ability of *Mycobacterium avium* to grow in murine macrophages. J. Immunol. 168:825–833.
24. Underhill, D. M. 2003. Macrophage recognition of zymosan particles. J. Endotoxin Res. 9:176–180.
25. Vergne, I., J. Chua, S. B. Singh, and V. Deretic. 2004. Cell biology of *Mycobacterium tuberculosis* phagosome. Annu. Rev. Cell Dev. Biol. 20:367–394.
26. Vergne, I., R. A. Fratti, P. J. Hill, J. Chua, J. Belisle, and V. Deretic. 2004. *Mycobacterium tuberculosis* phagosome maturation arrest: mycobacterial phosphatidylinositol analog phosphatidylinositol mannoside stimulates early endosomal fusion. Mol. Biol. Cell 15:751–760.
27. Xu, S., A. Cooper, S. Sturgill-Koszycki, T. van Heyningen, D. Chatterjee, I. Orme, P. Allen, and D. G. Russell. 1994. Intracellular trafficking in *Mycobacterium tuberculosis* and *Mycobacterium avium*-infected macrophages. J. Immunol. 153:2568–2578.
28. Yates, R. M., and D. G. Russell. 2005. Phagosome maturation proceeds independently of stimulation of toll-like receptors 2 and 4. Immunity 23:409–417.